# Molding and Stretched Evolution of Optical Solitons in Cumulative Nonlinearities

Cesare Dari-Salisburgo,[1,2] Eugenio DelRe,[1,2,*] and Elia Palange[3,4]

[1]*Dipartimento di Fisica, Università dell'Aquila, 67010 L'Aquila, Italy*

[2]*Istituto Nazionale Fisica della Materia, Unità di Roma "La Sapienza", 00185 Rome, Italy*

[3]*Dipartimento di Ingegneria Elettrica, Università dell'Aquila, 67040 Monteluco di Roio (L'Aquila), Italy*

[4]*Istituto Nazionale Fisica della Materia, Unità dell'Aquila, 67010 L'Aquila, Italy*

(Received 1 April 2003; published 29 December 2003)

The observation of initial time dynamics of self-trapping in photorefractive media indicates that optical spatial solitons supported by intense cumulative nonlinearities manifest temporally nonlocal signatures in the form of stretched exponential behavior. This general result, supported also by numerical predictions, is triggered by wave shaping in a time-constant buildup map, a consequence of the spatially resolved inertial response intrinsic to the geometrical transition from a diffracting to a self-focused beam, inherent to soliton appearance.

DOI: 10.1103/PhysRevLett.91.263903 PACS numbers: 42.65.Tg, 42.65.Sf

Space-time effects appear as a general behavior when transient and strongly inhomogeneous systems are considered, and nonlocal equations intervene. In optics, cumulative/inertial processes are at once responsible for the enhanced optical nonlinearity and the characteristically slow time scales [1,2], features that pair, for example, the diverse phenomenology of thermal [3], photorefractive [4], and liquid crystal [5] self-action. Although in the vast majority of conventional schemes, such as grating/hologram formation and two-wave-mixing experiments, an effective local time response is observed, i.e., the material index of refraction evolution depends only on the particular position considered [4], the driving cumulative nonlinearity intrinsically involves a temporally nonlocal buildup process of light induced self-action, i.e., a time evolution which depends on the previous history of the process in different positions, through an integrodifferential relationship [6]. In these conventional schemes, the growth/decay process is characterized by a single time scale exponential, a behavior that is fully justified in the so-called small modulation depth limit [4]. For spatial solitons [7], in turn, cumulative dynamics play a different and more complex role, on which we presently intend to investigate. Traces of this permeate soliton phenomenology, from the life cycle of quasi-steady-state photorefractive solitons [8] to the self-trapping of incoherent and multimodal beams [2]. Here, experiments for conditions in which the incoherent/multimodal self-trapping supersedes specklelike filamentation indicate a more elaborate inertial smearing of space-charge fluctuations, that mediate self-action, even before an averaged response is reached [9]. Further evidence of this can be found in the appearance of multipattern oscillation, quite different from a time-averaged behavior, when the driving bias field is appropriately modulated in time [10], and more recently in the identification of space-time effects in modulation instability [11]. Whereas the model of the dynamics has been in part formulated [12,13], the phenomenology and, hence, the physical behavior of the transient formation stage of solitons has remained hereto unknown. By experimentally investigating, for the first time, the initial stage of cumulative soliton formation, we find a temporal behavior completely different from known phenomena, characterized by substantial discriminating observable effects (nonlocal signatures) whenever the linear diffraction length is considerably smaller than the propagation length, i.e., when operatively a spatial soliton emerges [14]. This substantiates the fact that the very *nature* of self-trapping involves *spatiotemporal nonlocality*. We thus address, through a comparative experiment, the most basic and fundamental issue: What condition specific to soliton formation triggers this nonlocality, and what direct general signatures indicate its appearance? In particular, can it be ascribed to a simple consequence of a large intensity modulation depth, the basis for a local response in wave-interference schemes, or does it derive from direct spatiotemporal coupling, i.e., from the progressive change of beam shape along the transverse and longitudinal axes?

In cumulative processes, the time constant is point dependent through the intensity spatial distribution. For an initially diffracting wave, this leads to an underlying time-constant map that contributes to the overall beam manifestation. Results in photorefractive crystals indicate that this map triggers inertial signatures which are therefore intrinsic to the basic topological deformation associated with solitons. Results are compatible with the idea that the nonlocal signature comes from the superimposed appearance of a continuum of different exponential decays, resulting in a single stretched exponential behavior. Numerical results support this thesis and show that experimental findings are incompatible with a time dependent, but local, approach, in contrast to what was previously believed [15].

Photorefractive self-action is mediated by the formation of a light driven space-charge field that changes

  

beam evolution by electro-optically modifying the local index of refraction. In the 1 + 1D band-transport model, the (slow) time scales involved are associated with the formation of an $x$-directed space charge $E_{sc}(x, z, t)$, in response to an $x$-polarized optical field $E(x, z, t)$, $z$ axis corresponding to the beam-propagation direction. $E_{sc}$ obeys the cumulative equation [4,13]

$$\frac{\partial E_{sc}}{\partial t} + \frac{1}{\tau_d}\left(1 + \frac{I}{I_b}\right)E_{sc} = \frac{E_0}{\tau_d}, \tag{1}$$

which closes the Band-transport photorefractive model for conditions in which displacement charge, diffusion [16], and photovoltaic effects can be neglected, i.e., in the screening slab-soliton-supporting regime [17]. In Eq. (1), $\tau_d = \epsilon_0\epsilon_r\gamma N_a/[q\mu s(N_d - N_a)I_b]$ is the so-called dielectric time constant, $\gamma$ is the recombination rate, $N_a$ is the density of acceptor impurities, $N_d$ is that of donors, $q$ is the electron charge, $\mu$ is the electron mobility, $s$ is the donor impurity photoionization efficiency, $I_b$ is the equivalent background illumination, $I(x, z, t) = |A|^2$, $A$ is the slowly varying part of $E$, $E_0 = V/L$, $V$ is the bias voltage, and $L$ is the distance between the crystal electrodes along the $x$ axis. Evidently, the cumulative Eq. (1) reduces to the local nonlinearity (the screening soliton saturated Kerr nonlinearity in our case) in the steady-state regime [17], but the transient structure is characterized by a nonlocal relationship between $E_{sc}$ and $I$, with $A$ related to the index modulation $\Delta n(E_{sc})$ through the parabolic equation $[\partial_z + (i/2k)\partial_{xx}]A = (-ik/n)\Delta nA$ [4,13], $k$ being the wave vector and $n$ the unperturbed sample refractive index. The strong link between solitons and time (as opposed to space) nonlocality is evidenced by the fact that the two basic conditions that reduce Eq. (1) to a *local* dynamical evolution are *incompatible with self-trapping*. The first is the small modulation linearized limit, i.e., $I \ll I_b$, in which the nonlinear coupling between $I$ and $E_{sc}$ gives a negligible contribution. In contrast, solitons stem from large modulation (in general $I \geq I_b$) [17]. The second condition is when $I$ is only weakly time and space dependent [15]. Valid for holographic/grating schemes, it is equally incompatible with solitons which evolve from a diffracting wave $I(x, z, t = 0)$ into a self-trapped beam $I_{\mathrm{sol}}(x) \neq I(x, z, t = 0)$ independent of $z$ and $t$.

Our investigation proceeds through a series of experiments carried out in a zero-cut $3.7^{(x)} \times 4.1^{(y)} \times 2.4^{(z)}$ mm sample of paraelectric potassium-lithium-tantalate-niobate (KLTN), which can support photorefractive slab solitons through the screening nonlinearity [18], along with diffusion-driven [19] and spontaneous [20] self-action. The sample is photorefractive through copper and vanadium impurities and has $n = 2.2$. Although in the paraelectric phase the nonlinear response occurs through the quadratic electro-optic effect, with electro-optic coefficient $g_{\mathrm{eff}} = 0.12m^4C^{-2}$, findings refer to the entire family of photorefractive solitons, because the nonlocal mechanism resides in the cumulative inertial processes of Eq. (1). Furthermore, in the endeavor of finding general inertial signatures in the initial transient formation segments, we encounter no fundamental distinction between quasi-steady-state [8] and steady-state self-trapping [17]. Our findings refer to the quasi-steady state, thus allowing the evaluation of the role of modulation depth, comparing soliton formation for a large range of soliton intensity ratios $u_0^2 = I_p/I_b$ ($I_p$ is the input beam peak intensity) well beyond the region in which steady-state solitons can be reasonably achieved [17,18].

The setup conforms to the standard 1 + 1D slab soliton supporting scheme [17,18]. The input, approximately one-dimensional $x$-polarized (parallel to the external bias $E_0$) fundamental Gaussian beam, obtained appropriately from a $\lambda = 514$ nm CW $Ar^+$ laser, was focused onto the input facet of the sample to a spot size having an intensity at full width half maximum (FWHM) $\Delta x_{\mathrm{in}}$, determining the diffraction scale $\ell_d$. Beam power at the input crystal facet is of the order of tens of $\mu$W, depending on the particular conditions studied. Soliton propagation is obtained by fixing the physical parameters, i.e., the background intensity $I_b$, obtained in the conventional manner by launching a copropagating $y$-polarized plane wave [17], and, for the given crystal temperature $T = 25\,^{\circ}\mathrm{C}$, stabilized through feedback Peltier circuit (corresponding to $\epsilon_r \simeq 8.5 \times 10^3$), the value of $E_0$ [18]. Peculiarities of the KLTN soliton supporting scheme can found in Ref. [18]. The temporal evolution towards a trapped configuration of the output intensity distribution is captured in real time by imaging the output facet of the sample onto the CCD camera, equipped with fast electronics that provides $\Delta x$ versus time. As the initially diffracting beam molds its index pattern, the output FWHM $\Delta x_{\mathrm{out}}$ passes from its freely diffracting value $\Delta x_{\mathrm{out}}(t = 0) = \Delta x_{\mathrm{in}}\sqrt{1 + (\ell_z/\ell_d)^2}$, to the self-trapped plateau value $\Delta x_{\mathrm{out}}(t > \tau_s) \simeq \Delta x_{\mathrm{in}}$, where $\tau_s$ is the characteristic time scale (see below) [4].

The evaluation of time dynamics is susceptible to spurious beam distortion typical of modulation and snake instabilities [21], apart from transverse intensity inhomogeneities. For the given $\Delta x_{\mathrm{in}}$, we have set $E_0$ such as to obtain steady-state self-trapping for $u_0^2 \simeq 1$. Corresponding to the lowest nontransient supporting field, it gave rise to transient undistorted self-trapping for $u_0^2 > 1$.

We begin by evaluating the role played by temporal coupling. The geometrical feature can be isolated by comparing the self-trapping process in conditions of *weak* and *strong* $z$ dynamics. In Fig. 1 we show the comparison of soliton time evolution between these two basic regimes: the first obtained when the diffraction scale $\ell_d$ is comparable to the propagation distance $\ell_d \sim \ell_z = 2.4$ mm, and the second when it is considerably smaller.

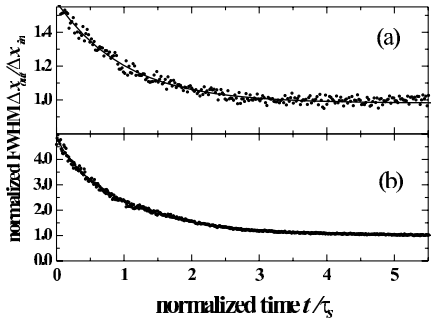


FIG. 1. Soliton formation for weak (a) and strong (b) $z$ dynamics in the collapsing stage ($\tau_s \ll \tau_d$). The continuous lines are the exponential (a) and stretched exponential fit ($\beta = 0.89$) (b).

In Fig. 1(a), we show typical soliton dynamics for $\ell_z/\ell_d = 1.16$ , obtained by launching a $\Delta x_{\rm in} = 14\ \mu$m beam, for an intensity ratio $u_0^2 = (9)^2$, with an applied field of $E_0 = 1.2$ kV/cm. The results of the comparative experiments shown in Fig. 1(b) refer to the second class of strong $z$ dynamics, where we have set $\Delta x_{\rm in} = 6.5\ \mu$m, leading to $\ell_z/\ell_d = 5.4$, setting again $u_0^2 = (9)^2$, and appropriately rescaling the bias field to $E_0 = 2.5$ kV/cm.

For the case of Fig. 1(a), $I$ is only weakly dependent on $t$ during the transient, and we can predict from Eq. (1) an approximate exponential evolution $\Delta x_{\rm out}(t) = [\Delta x_{\rm out}(0) - \Delta x_{\rm in}]e^{-t/\tau_s} + \Delta x_{\rm in}$, characterized by a single time scale $\tau_s$, substantiating a local time evolution. Reflecting the cumulative process of a standard buildup, space-charge temporal dynamics are *independent* of propagation effects: The dynamics of a "slice" of crystal at a given $z$ do not depend on the dynamics of a previous slice at a $z' < z$ (locality). Accordingly, data analysis indicates that an exponential decay fits the experimental data. Conversely, this is not the case for the time evolution curve of Fig. 1(b). Here, time behavior is fitted and described by a *stretched exponential*, i.e., by a decay that follows $e^{-(t/\tau_s)^\beta}$, with $\beta < 1$, a qualitatively different time evolution that characterizes spatial soliton formation.

In order to evaluate the validity and nature of this phenomenological signature, we repeated the comparison for a large range of values of $u_0^2$, for both regimes, scanning a variety of conditions and isolating the role of modulation depth that depends on $u_0^2$.

Results in the strong $z$-dynamics regime are shown in Fig. 2, where the values of the measured stretching exponent $\beta$ as a function of soliton $u_0^2$ are plotted. Again, the most striking feature is the consistency of the signature for the entire range of soliton phenomenology (i.e., for $\ell_z/\ell_d = 5.4$), for which the best fit value is always $\beta < 1$. In other words, the stretched exponential transient regime is observed for all values of investigated modulation depth.

In the same conditions, we repeated the comparative experiment in the weak $z$-dynamics regime and obtained a consistent fit with a single exponential decay (i.e., $\beta = 1$). The use of the full nonlinear model does not appreciably ameliorate the fit, which in any case does not manifest any stretching ($\beta \gtrsim 1$, i.e., the evolution is fundamentally different from the previous case).

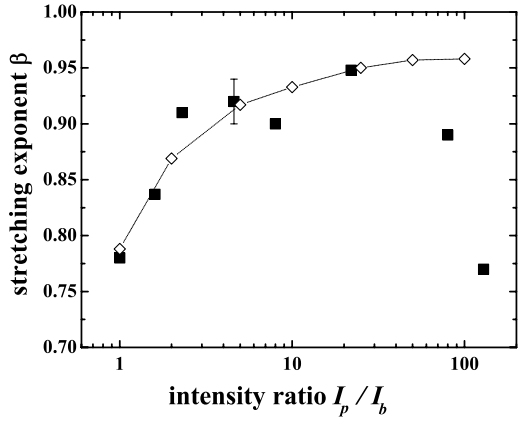


FIG. 2. Soliton time stretching vs $u_0^2$ (squares), compared to the numerical prediction (diamonds).

Apart from stretching, associated to the shaping of the spatial soliton, Fig. 2 shows that the value of $\beta$ depends on the intensity modulation in the soliton regime.

Stretching has the nontrivial feature of relegating the "distortion" to a single *dimensionless* parameter: We do not expect the appearance of specific new scales and the basic time structure which undergoes stretching should derive from the local version of Eq. (1); i.e., the product $I\tau$ is constant. We thus analyzed the observed time constants for the cases of Fig. 2. The measured values of $I_p\tau_s$ are shown in Fig. 3. Results confirm, at least for $u_0^2 > 10$, the validity of the $\tau_s \propto I^{-1}$ law, and thus that no new time scales appear, whereas in the low intensity regime, as already evidenced in Fig. 2, the differentiation from the local prediction $I_p\tau_s = \tau_d I_b u_0^2/(1 + u_0^2)$ is accentuated (note that, as defined above, $\tau_d \propto I_b^{-1}$). Experimental

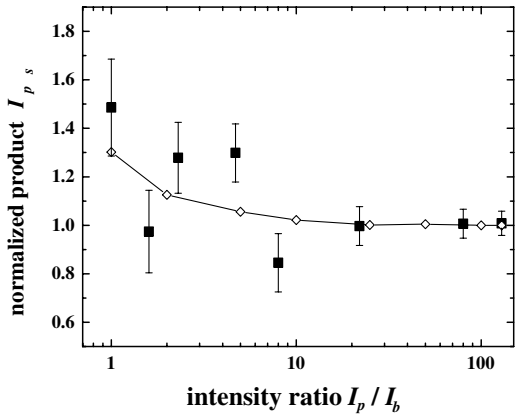


FIG. 3. Validity of $\tau_s \propto I^{-1}$ for $u_0^2 > 10$. Squares (diamonds) are the measured (predicted) values.

uncertainty is the effect of the spatial inhomogeneities in $I_b$ (especially along the second transverse direction, orthogonal to $x$), which for medium and large values of $u_0^2$ have little impact. For $u_0^2 = 22$ and $I_p = 3\ \mathrm{kW/m^2}$, $\tau_s = 200$ s, and $\tau_d \simeq u_0^2 \tau_s$. The value of $u_0$ was varied by changing $I_b$ (always larger than the dark illumination), hence, $\tau_d$ varies for each measurement.

We conclude that in Eq. (1) stretching is a consequence of the fact that, for each given $z$, evolution has a different $\tau(z) \simeq \tau_d(1 + I/I_b)^{-1}$, the picture complicated by the fact that the time constants themselves *evolve*. Whereas we cannot explicitly predict the outcome of the superposition, we find it fully compatible with the observed behavior. Our understanding has a precise consequence: The formation time is independent of the ratio $\ell_z/\ell_d$ (i.e., the sample or propagation length). This excludes alternative intuitive mechanisms, consisting in the formation of a self-trapped planar-phase wave condition that progressively forms (in space and time) cascading along the beam-propagation axis, as could occur for a thresholdlike nonlinearity.

We have carried out a time-dependent beam-propagation analysis, using a time step integration of Eq. (1) and the propagation equation [22]. We find good agreement with measured results for all regimes except for large values of $u_0^2$ (Fig. 2). Equation (1) describes the relatively general class of buildup mechanisms in which time scales are proportional to local light intensity, a feature which translates into universal $\beta$ vs $u_0^2$ (Fig. 2) characteristics for a given propagation equation [Eq. (1) can be directly normalized into $\partial_{t'} E' + (1 + u^2)E' = 1$, where $t' = t/\tau_d$, $E' = E_{sc}/E_0$, and $u^2 = I/I_b$]. The discrepancy heralds the onset of system-dependent features that break this down (though not affecting the $\tau_s \propto I^{-1}$ law). In our particular case, the impact of displacement charge [7,17] increases at high intensity ratio, and a first correction can be obtained by multiplying the second term on the left-hand side of Eq. (1) by $[1 - \epsilon \nabla E_{sc}/(N_a q)]$.

Stretching, which originates from the geometrical time map *intrinsic* to spatial soliton formation, implies that during transients we are never entitled to substitute the fully nonlocal cumulative evolution of Eq. (1) (whose explicit expression can be found in [13]), or its equivalent for other thermal/reorientational buildup mechanisms, with the more ambiguous, but local, expression [15] $E_{sc} = E_0 \exp[-(1 + \bar{I}/I_b)t/\tau_d](1 + \{\exp[(1 + \bar{I}/I_b)t/\tau_d] - 1\}/(1 + \bar{I}/I_b))$, where $\bar{I}$ is the average intensity on a characteristic (fast) time scale.

In conclusion, we have investigated, for the first time, dynamics of spatial self-trapping when relevant propagation dynamics are present, i.e., for a regime that allows the appearance of solitons. What emerges is a highly time-nonlocal evolution, characterized by stretching, that constitutes an optical embodiment of an intrinsic manifestation of nonlocal effects in transient and inhomogeneous systems.

This research was funded by the Italian Istituto Nazionale Fisica della Materia (INFM) through the "Solitons embedded in holograms" (SEH) project, and by the Italian Ministry of Research through the "Space-time effects" PRIN 2001 and FIRB 2002 projects.

*Electronic address: eugenio.delre@aquila.infn.it

[1] E. V. Doktorov and R. A. Vlasov, Europhys. Lett. **26**, 487 (1994).
[2] M. Mitchell, M. Segev, and D. N. Christodoulides, Phys. Rev. Lett. **80**, 4657 (1998); M. Mitchell and M. Segev, Nature (London) **387**, 880 (1997).
[3] E. V. Doktorov *et al.*, Phys. Lett. A **157**, 181 (1991); D. Kip *et al.*, Opt. Lett. **23**, 343 (1998); J. S. Hammonds *et al.*, Opt. Commun. **194**, 47 (2001).
[4] L. Solymar, D. J. Webb, and A. Grunnet-Jepsen, *The Physics and Applications of Photorefractive Materials* (Clarendon, Oxford, 1996).
[5] E. Braun *et al.*, Europhys. Lett. **23**, 239 (1993); M. F. Shih and F. W. Sheu, Opt. Lett. **24**, 1853 (1999); M. Peccianti and G. Assanto, Phys. Rev. E **65**, 35603 (2002).
[6] Temporal nonlocality is an effect along the propagation axis distinct from transverse diffusion mechanisms.
[7] *Spatial Solitons*, edited by S. Trillo and W. Torruellas (Springer-Verlag, Berlin, 2001).
[8] G. C. Duree *et al.*, Phys. Rev. Lett. **71**, 533 (1993).
[9] M. F. Shih and F. W. Sheu, Phys. Rev. Lett. **86**, 2281 (2001).
[10] G. M. Tosi-Beleffi *et al.*, Opt. Lett. **25**, 1538 (2000).
[11] M. F. Shih *et al.*, Phys. Rev. Lett. **88**, 133902 (2002).
[12] A. A. Zozulya and D. Z. Anderson, Opt. Lett. **20**, 837 (1995).
[13] B. Crosignani *et al.*, J. Opt. Soc. Am. B **14**, 3078 (1997).
[14] New physics emerges during a strong collapsing stage for times much shorter than the dielectric relaxation time $\tau_d$.
[15] See, for example, N. Fressengeas, J. Maufoy, and G. Kugel, Phys. Rev. E **54**, 6866 (1996).
[16] In thermal and polymeric media, diffusion can play a role, and must be taken into account in Eq. (1).
[17] M. Segev *et al.*, Phys. Rev. Lett. **73**, 3211 (1994); D. N. Christodoulides and M. I. Carvalho, J. Opt. Soc. Am. B **12**, 1628 (1995); M. Segev, M. Shih, and G. C. Valley, J. Opt. Soc. Am. B **13**, 706 (1996).
[18] E. DelRe *et al.*, Opt. Lett. **23**, 421 (1998).
[19] B. Crosignani *et al.*, Phys. Rev. Lett. **82**, 1664 (1999).
[20] E. DelRe *et al.*, Phys. Rev. Lett. **83**, 1954 (1999).
[21] A. V. Mamaev *et al.*, Europhys. Lett. **35**, 25 (1996).
[22] As in Ref. [9], $10^3$ iterations for a $2\tau_s$ window with 50 $z$ and $2.5 \times 10^3$ $x$ steps ($\Delta z = 48\ \mu$m, $\Delta x = 0.6\ \mu$m).